A Near-Optimal Model-Based Control Algorithm for Households Equipped With Residential Photovoltaic Power Generation and Energy Storage Systems

Yanzhi Wang, *Student Member, IEEE*, Xue Lin, *Student Member, IEEE*, and Massoud Pedram, *Fellow, IEEE*

***Abstract*—Integrating residential photovoltaic (PV) power generation and energy storage systems into the Smart Grid is an effective way of reducing fossil fuel consumptions. This has become a particularly interesting problem with the introduction of dynamic electricity energy pricing, since consumers can use their PV-based energy generation and controllable energy storage devices for peak shaving on their power demand profile, thereby minimizing their electricity bill. A realistic electricity pricing function is considered with billing period of a month, comprising both an energy price component and a demand price component. Due to the characteristics of electricity price function and energy storage capacity limitation, the residential storage control algorithm should 1) utilize PV power generation and load power consumption predictions and 2) account for various energy loss components during system operation, including energy loss components due to rate capacity effect in the storage system and power dissipation of the power conversion circuitry. A near-optimal storage control algorithm is proposed accounting for these aspects. The near-optimal algorithm, which controls the charging/discharging of the storage system, is effectively implemented by solving a convex optimization problem at the beginning of each day with polynomial time complexity. For further improvement, the reinforcement learning technique is adopted to adaptively determine the residual energy in the storage system at the end of each day in a billing period.**

***Index Terms*—Energy storage, optimal control, photovoltaic, reinforcement learning.**

I. Introduction

THE traditional static and centralized structure of electricity grid (a.k.a. the power grid) comprised a transmission network, which transmits electrical power generated at remote power plants through long-distance high-voltage lines to substations, and a distribution network, which delivers electrical power from substations to local end users/consumers. In this infrastructure, the local distribution network is often statically adjusted to match the load profile of its end users. Since the end user profiles often change considerably according to the day of week and time of day, the power grid must be able to support the worst-case power demands of all the end users at all times in order to avoid potential power delivery failure (blackout or brownout) [2].

The decentralized *Smart Grid* infrastructure is being designed to avoid expending a large amount of capital for increasing the power generation capacity of utility companies in order to meet the expected growth of end user energy consumptions in the worst case [3], [4]. The Smart Grid is also being equipped with smart meters, which can monitor and control the power flow in the power grid to match the amount of power generation to power consumption, and to minimize the overall cost of electrical energy delivered to end users.

In the Smart Grid infrastructure, utility companies can employ *dynamic electricity pricing* strategies, i.e., employing different electricity prices at different time periods in a day or at different locations. This policy can incentivize consumers to perform *demand side management*, by adjusting their power demand from the Grid to match the power generation capacity of the Grid. There are several ways to perform such a demand side management, including integration of intermittent energy sources such as photovoltaic (PV) power or wind power at the residential level, demand shaping (i.e., consumers shift their tasks to the off peak periods), household task scheduling, etc. [5]. In this paper, we focus on the former solution, or more specifically, integrating PV power generation with the Smart Grid for residential usage.

Although integrating residential renewable energy sources into the Smart Grid proves to be an effective way of utilizing renewable power and reducing the consumption of fossil fuels, several problems need to be addressed for these benefits to be realized. First, there exists a mismatch between the peak PV power generation time (usually at noon) and the peak load power consumption time for residential users (usually in the evening) in each day [6]. This timing skew results in conditions where the generated PV power cannot be optimally utilized for peak power shaving. Moreover, at each time instance, the PV output power is fixed depending on the solar irradiance, and by employing the maximum power point tracking (MPPT) or maximum power transfer tracking (MPTT) control methods [10], [11]. Hence, the ability of the residential user for peak shaving is also restricted by PV output power.

One effective solution to the aforementioned problems is to incorporate energy storage systems, either homogeneous or hybrid, into the PV-assisted Smart Grid infrastructure for residential users [1], [6]–[9]. The proposed residential energy storage system shall store power from the Smart Grid during off peak periods of each day and (or) from the PV system, and

Manuscript received January 03, 2015; revised May 27, 2015; accepted July 07, 2015. Date of publication September 23, 2015; date of current version December 11, 2015. This work was supported by a grant from the National Science Foundation. A preliminary version of this paper was presented at the 2013 IEEE Green Technologies Conference (GreenTech), Denver, CO, USA, 2013. Paper no. TSTE-00006-2015.

The authors are with the Department of Electrical Engineering, University of Southern California, Los Angeles, CA 90089 USA (e-mail: yanzhiwa@usc.edu; xuelin@usc.edu; pedram@usc.edu).

Color versions of one or more of the figures in this paper are available online at http://ieeexplore.ieee.org.

Digital Object Identifier 10.1109/TSTE.2015.2467190

provide power for the end users during the peak periods of that day for peak power shaving and energy cost reduction (since electrical energy tends to be the most expensive during these peak hours). Therefore, the design of energy pricing-aware control algorithm for the residential storage system, which controls the charging and discharging of energy storage bank(s) and the magnitude of charging/discharging current, is an important task in order for the Smart Grid technology to deliver on its promises.

Effective storage control algorithms should take into account the realistic electricity pricing function, such as [12] and [13]. It comprised both an *energy price* component, which is a time-of-usage (TOU)-dependent function indicating the unit energy price during each time period of the billing period (a day, or a month, etc.). The actual deployment [12] uses a month as the billing period, and a *demand price* component, which is an additional charge due to the peak power consumption in the billing period. The latter component is required in order to prevent a case whereby all the customers utilize their PV power generation and energy storage systems and/or schedule their loads such that a very large amount of power is demanded from the Smart Grid during low-cost (off peak) time slots, which can subsequently result in power delivery failure for the end users.

The capacity of the storage system is limited due to the relatively high cost of electrical energy storage elements. Therefore, the following two requirements need to be satisfied so that the storage controller can perform optimization of the total cost induced by both the energy price and the demand price. First, at each decision epoch of a billing period, it is important for the controller to forecast the PV power generation and load power consumption profiles. Second, the storage control algorithm should accurately account for the energy loss in the storage charging/discharging process and in power conversion circuitry to achieve optimality in total cost saving. This requirement implies taking into account accurate energy loss models for storage and power conversion circuitry in the controller's optimization framework. To satisfy the first requirement, Refs. [14]–[18] are representatives of general PV power generation and load power consumption predictions by either forecasting the complete power profiles or certain statistical characteristics of the power profiles. In [6], we have presented PV and load power profiles prediction algorithms specifically designed for a Smart Grid residential user. On the other hand, few research papers have focused on addressing the second requirement.

In this paper, we consider the case of a Smart Grid residential user equipped with local PV power generation and an energy storage system. We consider realistic electricity price function composed of both energy and demand prices, with the billing period of a month [12]. We first provide the overall system architecture and the storage power loss model used in the paper. Based on the PV power generation and load power consumption prediction results from previous papers, we present a near-optimal storage control algorithm that properly accounts for the energy loss components due to power dissipation in the power conversion circuitries, as well as the rate capacity effect, which is the most significant portion of energy loss in the storage system. The proposed near-optimal storage control algorithm is effectively implemented by solving a convex optimization problem with polynomial time complexity at the beginning of each day in a billing period. Moreover, we adopt reinforcement learning technique [24] to adaptively determine the amount of residual energy in the energy storage module at the end of each day in a billing period. Experimental results demonstrate that the proposed residential storage control algorithm achieves up to $2.91\times$ (i.e., 191% higher) enhancement in electricity cost reduction compared with baseline storage control algorithm.

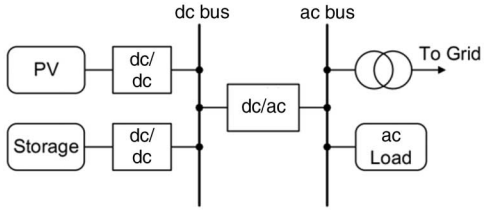

Fig. 1. Block diagram showing the interface between PV module, storage system, residential load, and the Smart Grid.

The proposed algorithm is "near-optimal" in the following senses: we cannot find the optimal solution of storage control over the whole billing period (a month) because we cannot have (PV and load) prediction results over a month. Hence, we find a near-optimal solution by deriving the optimal storage control over the subsequent day and keeping a certain amount of residue energy at the end of that day. We optimally solve the storage control problem for the subsequent day, and use reinforcement learning technique to derive the optimal residue energy. The reinforcement learning technique will converge to the true optimal solution under certain circumstances, e.g., learning rate gradually decreases and the learning period is an infinite horizon [24].

The remainder of this paper is organized as follows. We describe the system modeling, price function, and overall cost function in Section II. Section III presents the power loss model of the storage system. Section IV presents the residential storage control algorithm to minimize the total energy cost over a billing period. Experimental results and conclusion are presented in Sections V and VI, respectively.

II. System Modeling and Cost Function

In this paper, we consider an individual Smart Grid residential user equipped with PV power generation and energy storage systems, as shown in Fig. 1. The PV system and the storage system are connected to a *residential dc-bus*, via unidirectional and bidirectional dc–dc converters, respectively. An ac-bus, which is further connected to the Smart Grid, is connected via an ac/dc interface (e.g., inverter, rectifier, and transformer circuitry) to the residential dc-bus. The residential ac load (e.g., household appliances, lighting, and heating equipments) is connected to the ac bus. In this paper, we consider the power losses in the aforementioned power conversion circuitry for realistic concern.

We adopt a *slotted time* modeling approach, i.e., all system constraints as well as decisions are provided for discrete time intervals of equal and constant length. More specifically, each day is divided into T time slots, each with a duration of D. We

use $T = 96$ and $D = 15$ min. Set $\boldsymbol{S}$ will denote the set of all T time slots in each day.

We adopt a realistic electricity price function composed of both the energy price component and the demand price component as discussed before, with a billing period of a month [12]. Consider a specific day i of a billing period. The residential load power consumption at the jth time slot of that day is denoted by $P_{\text{load},i}[j]$. The output power levels of PV and storage systems at the jth time slot are denoted by $P_{\text{pv},i}[j]$ and $P_{\text{st},i}[j]$, respectively. Notice that, $P_{\text{st},i}[j]$ may be positive (discharging from the storage), negative (charging the storage), or zero.

We assume that the PV power generation $P_{\text{pv},i}[j]$ and residential load power consumption $P_{\text{load},i}[j]$ can be accurately predicted at the beginning of the ith day. We use $P_{\text{grid},i}[j]$ to denote the power required from the Smart Grid, i.e., the *grid power*, at the jth time slot of the ith day, where $P_{\text{grid},i}[j]$ can be positive (if the Smart Grid provides power for the residential usage), negative (if the residential system sells power back into the Smart Grid), or zero. More accurately, such as $P_{\text{load},i}[j]$, $P_{\text{pv},i}[j]$, $P_{\text{st},i}[j]$, and $P_{\text{grid},i}[j]$ values can be viewed as the average power generation or consumption values in the jth time slot of the ith day.

We consider realistic power conversion circuitry (i.e., their power conversion efficiency is less than 100%) in the proposed optimization framework. Accordingly, we use η_1, η_2, and η_3 to denote the power conversion efficiencies of the dc–dc converter between the PV system and the dc-bus, the dc–dc converter connecting between the storage system and the dc-bus, and the ac/dc power conversion interface, respectively. Those power conversion efficiency values are typically in the range of 85%–95%. Note that the conversion efficiency is quite stable for a high-power converter in a wide range of load current levels [26], [27].

There are three *operating modes* in the system. In the first mode, both the PV system and the storage system are providing power for the residential load (i.e., the storage system is being discharged). For the jth time slot of the ith day, the condition that the residential system is in the first mode is given by $P_{\text{st},i}[j] \geq 0$. In this case, the actual grid power $P_{\text{grid},i}[j]$ can be calculated by

$$P_{\text{grid},i}[j] = P_{\text{load},i}[j] - \eta_1 \cdot \eta_3 \cdot P_{\text{pv},i}[j] - \eta_2 \cdot \eta_3 \cdot P_{\text{st},i}[j]. \quad (1)$$

In the second mode, the storage system is being charged, and the PV system is sufficient for charging the storage. For the jth time slot of the ith day, the condition that the residential system is in the second mode is given by $P_{\text{st},i}[j] < 0$ and $\eta_1 P_{\text{pv},i}[j] + \frac{1}{\eta_2} P_{\text{st},i}[j] \geq 0$. In this mode, there is power flowing from the dc-bus to the ac bus, and the actual grid power can be calculated by

$$P_{\text{grid},i}[j] = P_{\text{load},i}[j] - \eta_1 \eta_3 \cdot P_{\text{pv},i}[j] - \frac{\eta_3}{\eta_2} \cdot P_{\text{st},i}[j]. \quad (2)$$

In the third mode, the storage system is being charged, and the PV system is insufficient for charging the storage. In other words, the storage is simultaneously charged by the PV system and the Grid. For the jth time slot of the ith day, the condition that the residential system is in the third mode is given by $P_{\text{st},i}[j] < 0$ and $\eta_1 P_{\text{pv},i}[j] + \frac{1}{\eta_2} P_{\text{st},i}[j] < 0$. In this mode, there is power flowing from the ac-bus to the dc-bus, and the actual grid power is given by

$$P_{\text{grid},i}[j] = P_{\text{load},i}[j] - \frac{1}{\eta_3} \cdot \left(\eta_1 P_{\text{pv},i}[j] + \frac{1}{\eta_2} P_{\text{st},i}[j] \right). \quad (3)$$

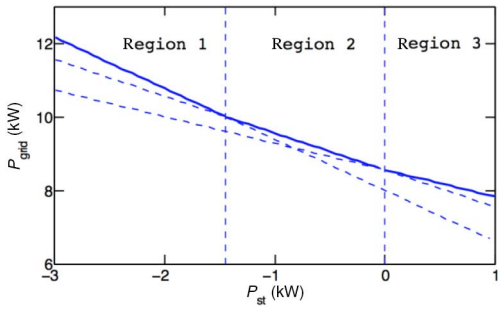

Fig. 2. Illustration of the relationship between $P_{\text{grid},i}[j]$ and $P_{\text{st},i}[j]$.

Each of equations (1)–(3) is a linear and monotonically decreasing function of $P_{\text{st},i}[j]$ when $P_{\text{pv},i}[j]$ and $P_{\text{load},i}[j]$ values are given. Fig. 2 provides an illustration of the relationship between $P_{\text{grid},i}[j]$ and $P_{\text{st},i}[j]$. The relationship between $P_{\text{grid},i}[j]$ and $P_{\text{st},i}[j]$ satisfies (3) in region 1 ($\eta_1 P_{\text{pv},i}[j] + \frac{1}{\eta_2} P_{\text{st},i}[j] < 0$), satisfies (2) in region 2 ($P_{\text{st},i}[j] < 0$ and $\eta_1 P_{\text{pv},i}[j] + \frac{1}{\eta_2} P_{\text{st},i}[j] \geq 0$), and satisfies (1) in region 3 ($P_{\text{st},i}[j] \geq 0$). Thus, $P_{\text{grid},i}[j]$ is a piecewise linear and monotonically decreasing function of $P_{\text{st},i}[j]$. $P_{\text{grid},i}[j]$ is also a convex function of $P_{\text{st},i}[j]$ since the derivative of $P_{\text{grid},i}[j]$ with respect to $P_{\text{st},i}[j]$ is nondecreasing (as shown in Fig. 2).

As specified in [12] and [13], the electricity price function is preannounced by the utility company just before the start of each billing period, and it will not change until possibly the start of the next billing period. We use a general electricity price function as follows. We use $\text{Price}_E[j]$ to denote the unit energy price at the jth time slot of a day. Then the cost we actually pay in a billing period due to the energy price component is given by

$$\text{Cost}_E = \sum_{i=1}^{30} \sum_{j=1}^{96} \text{Price}_E[j] \cdot P_{\text{grid},i}[j] \cdot D. \quad (4)$$

The demand price component, on the other hand, is charged for the peak power drawn from the Grid over certain time periods in a billing period. A generic definition of the demand price is given as follows. Let $\boldsymbol{S}_1, \boldsymbol{S}_2, \ldots, \boldsymbol{S}_N$ be N different nonempty subsets of the original set $\boldsymbol{S}$ of time slots, each of which corresponds to a specific time period, named by the term *price period*, in a day. A price period does not necessarily need to be continuous in time. For example, a price period can span from 10:00 to 12:59 and then from 17:00 to 19:59, as shown in [12]. Also those price periods in a day do not need to be mutually exclusive. We use $j \in \boldsymbol{S}_k$ to denote the statement that the jth time slot in a day belongs to the kth price period. Let $\text{Price}_{D,k}$ denote the demand price charged over each kth price period $\boldsymbol{S}_k$. Then the cost we have to pay in a billing period due to the demand price component is given by

$$\text{Cost}_D = \sum_{k=1}^{N} \text{Price}_{D,k} \cdot \max_{1 \leq i \leq 30, j \in \boldsymbol{S}_k} P_{\text{grid},i}[j]. \quad (5)$$

Obviously, the actual total cost for the residential user in a billing period (i.e., a month) is the sum of the two aforesaid cost components.

III. Storage Power Model

The most significant cause of power losses in the storage system, which is typically made of lead-acid batteries or Li-ion batteries, is the rate capacity effect of batteries [19]. To be more specific, high discharging current of the battery will reduce the amount of available energy that can be extracted from the battery, thereby reducing the battery service life between fully charged and fully discharged states [19]. In other words, high-peak-pulsed discharging current will deplete much more of the battery's stored energy than a smooth workload with the same total energy demand. We use *discharging efficiency* of a battery to denote the ratio of the battery's output current to the degradation rate of its stored charge. Then the rate capacity effect specifies the fact that the discharging efficiency of a battery decreases with the increase of the battery's discharging current. The rate capacity effect also affects the energy loss in the battery during the charging process in a similar way.

The rate capacity effect can be captured using the Peukert's formula [19], an empirical formula specifying the battery charging and discharging efficiencies as functions of the charging current I_c and the discharging current I_d, respectively,

$$\eta_{\text{rate},c}\left(I_c\right)=\frac{1}{\left(I_c/I_{\text{ref}}\right)^{\alpha_c}},\quad \eta_{\text{rate},d}\left(I_d\right)=\frac{1}{\left(I_d/I_{\text{ref}}\right)^{\alpha_d}} \tag{6}$$

where α_c and α_d are Peukert's coefficients, and their values are typically in the range of 0.1–0.3 (we derive the α_c and α_d values from our actual battery measurements [21]); I_{ref} denotes the *reference current* of the battery, which is proportional to the battery's nominal capacity C_{nom}. Typically, I_{ref} is set to $C_{\text{nom}}/20$, indicating that it takes 20 h to fully discharge the battery using discharging current I_{ref}.[1]

We name I_c/I_{ref} and I_d/I_{ref} the battery's normalized charging current and normalized discharging current, respectively. Notice that the efficiency values $\eta_{\text{rate},c}\left(I_c\right)$ and $\eta_{\text{rate},d}\left(I_d\right)$ in (6) are greater than 100% if the magnitude of the normalized charging or discharging current is less than one, which implies that the aforementioned Peukert's formula is not accurate in this case. We modify the Peukert's formula such that the efficiency values $\eta_{\text{rate},c}\left(I_c\right)$ and $\eta_{\text{rate},d}\left(I_d\right)$ become equal to 100% if the magnitude of the normalized charging/discharging current is less than one. In other words, the battery suffers from no rate capacity effect in this case. $\eta_{\text{rate},c}\left(I_c\right)$ and $\eta_{\text{rate},d}\left(I_d\right)$ are still given by (6) if the magnitude of normalized charging/discharging current is greater than one.

We denote the increase/degradation rate of storage energy in the jth time slot of the ith day by $P_{\text{st,in},i}[j]$, which may be positive (i.e., discharging from the storage and the amount of energy decreases), negative (i.e., charging the storage and the amount of energy increases), or zero. The unit of $P_{\text{st,in},i}[j]$ will be similar to that of power since it denotes the increase/decrease rate of storage energy. Based on the modified Peukert's formula, the relationship between $P_{\text{st,in},i}[j]$ and the storage output power $P_{\text{st},i}[j]$ is given by[2]

$$P_{\text{st},i}[j]=\begin{cases}V_{\text{st}}\cdot I_{\text{st,ref}}\cdot\left(\frac{P_{\text{st,in},i}[j]}{V_{\text{st}}\cdot I_{\text{st,ref}}}\right)^{\beta_1}, & \text{if } \frac{P_{\text{st,in},i}[j]}{V_{\text{st}}\cdot I_{\text{st,ref}}}>1\\ P_{\text{st,in},i}[j], & \text{if } -1\le\frac{P_{\text{st,in},i}[j]}{V_{\text{st}}\cdot I_{\text{st,ref}}}\le 1\\ -V_{\text{st}}\cdot I_{\text{st,ref}}\cdot\left(\frac{|P_{\text{st,in},i}[j]|}{V_{\text{st}}\cdot I_{\text{st,ref}}}\right)^{\beta_2}, & \text{if } \frac{P_{\text{st,in},i}[j]}{V_{\text{st}}\cdot I_{\text{st,ref}}}<-1\end{cases} \tag{7}$$

where V_{st} is the storage terminal voltage and is supposed to be (near-) constant; $I_{\text{st,ref}}$ is the reference current of the storage system, which is proportional to its nominal capacity $C_{\text{st,nom}}$ given in ampere-hours (Ah). When comparing (6) with (7), we observe that the relationship between β_1, β_2 and α_d, α_c, i.e., $\beta_1=\frac{1}{1+\alpha_d}$ and $\beta_2=\frac{1}{1-\alpha_c}$. Coefficient β_1 is in the range of 0.8–0.9, whereas coefficient β_2 is in the range of 1.1–1.3.

One can observe that when the storage discharging (or charging) current is the same, the discharging (or charging) efficiency becomes higher (i.e., the rate capacity effect becomes less significant) when the nominal capacity of the storage system is larger.

We use function $P_{\text{st},i}[j]=f_{\text{st}}\left(P_{\text{st,in},i}[j]\right)$ to denote the relationship between $P_{\text{st},i}[j]$ and $P_{\text{st,in},i}[j]$. An important observation is that such a function is a concave and monotonically increasing function over the input domain $-\infty<P_{\text{st,in},i}[j]<\infty$, as shown in Fig. 3. The concavity of function $f_{\text{st}}\left(P_{\text{st,in},i}[j]\right)$ is a result from characteristics of (7), i.e., coefficient β_1 is smaller than one and coefficient β_2 is larger than one. Due to the monotonicity property, $P_{\text{st,in},i}[j]$ is also a monotonically increasing function of $P_{\text{st},i}[j]$, denoted by $P_{\text{st,in},i}[j]=f_{\text{st}}^{-1}\left(P_{\text{st},i}[j]\right)$. We can see from Fig. 3 that a lead-acid battery-based storage system has more significant energy loss due to rate capacity effect than a Li-ion battery-based storage system. However, the lead-acid battery-based storage system is more often deployed in real household scenarios due to cost considerations (the capital cost of lead-acid battery is only 100–200 \$/kWh, whereas that of Li-ion battery is >600 \$/kWh [20]).

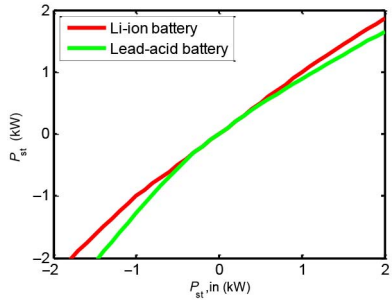

Fig. 3. Relationship between $P_{\text{st},i}[j]$ and $P_{\text{st,in},i}[j]$ in two types of batteries.

[1]Since I_{ref} is a very small current compared with battery capacity, it is typically safe to assume that the battery efficiency is close to 100% when charging/discharging using I_{ref}.

[2]Note that there is an absolute value calculation in the third term because $P_{\text{st,in},i}[j]$ is negative in this case. In the first term, $P_{\text{st,in},i}[j]$ is positive, and therefore, there is no need for the absolute value calculation.

IV. Optimal Control Algorithm of Residential Storage System

In this section, we introduce the proposed near-optimal residential storage control algorithm in detail, which could effectively utilize the combination of PV power generation and load power consumption prediction results to minimize the total electricity cost, including both the energy price and the demand price, over each billing period (i.e., a month).

The storage control optimization problem is performed at time 00:00 (i.e., at the beginning) of each day in the billing period. To be more realistic, we assume that the prediction results of PV power generation and load power consumption profiles at each ith day are not available before time 00:00 of that day. We further assume that the PV power generation and load power consumption profiles at each day, i.e., $P_{\text{pv},i}[j]$ and $P_{\text{load},i}[j]$ for $1 \le j \le 96$, can be accurately predicted from the weather forecast and prediction algorithms presented in our previous work [6]. At time 00:00 of each ith day, the storage controller performs optimization to find the optimal storage system output power profile $P_{\text{st},i}[j]$ for $1 \le j \le 96$ throughout the day, which is equivalent to finding the charging/discharging current profile of the storage system.

In this section, we first introduce the storage control optimization performed at the beginning of a billing period (i.e., at time 00:00 of day $i = 1$), in order to achieve a balance between the expected Cost_E (induced by the energy price component) and expected Cost_D (induced by the demand price component) values. In this way, we can minimize the total expected energy cost. Next, we introduce the storage control optimization performed at the beginning of the other days in the billing period. Finally, we provide a reinforcement learning technique [24] to adaptively determine the amount of residual energy in the energy storage module at the end of each day in a billing period.

Although in reality we control the output power $P_{\text{st},i}[j]$ ($1 \le i \le 30$, $1 \le j \le 96$) of the storage system during the system operation, we use $P_{\text{st,in},i}[j]$ ($1 \le i \le 30$, $1 \le j \le 96$) as the control variables in the optimal storage control problem formulation since it can help transform the optimal storage control problem into a standard convex optimization problem. We observe from (1), (2), (3), and (7) that the grid power $P_{\text{grid},i}[j]$ ($1 \le i \le 30$, $1 \le j \le 96$) is a monotonically decreasing function of $P_{\text{st,in},i}[j]$, denoted by $P_{\text{grid},i}[j] = f_{\text{grid}}\left(P_{\text{st,in},i}[j]\right)$, over the input domain $-\infty < P_{\text{st,in},i}[j] < \infty$. Again, we have $P_{\text{st,in},i}[j] = f_{\text{grid}}^{-1}\left(P_{\text{grid},i}[j]\right)$. Furthermore, $P_{\text{grid},i}[j] = f_{\text{grid}}\left(P_{\text{st,in},i}[j]\right)$ is a convex function of the control variable $P_{\text{st,in},i}[j]$ according to the rules of convexity in function compositions [22], due to the following two reasons: 1) $P_{\text{grid},i}[j]$ is a convex and monotonically decreasing function of $P_{\text{st},i}[j]$ and 2) $P_{\text{st},i}[j] = f_{\text{st}}\left(P_{\text{st,in},i}[j]\right)$ is a concave function of $P_{\text{st,in},i}[j]$.

At any time in a billing period, let Peak_k ($1 \le k \le N$) denotes the peak grid power consumption value that is *observed so far* over the kth price period in the billing period of interest (cf. Section II). Obviously, such Peak_k values are initialized to zero at the beginning of the billing period, and are updated at the end of each day according to the actual grid power consumption profiles.

At the beginning of the billing period, i.e., time 00:00 of day 1, the amount of energy stored in the storage system is $E_{\text{st,ini},1}$. The amount of stored energy at the beginning (time 00:00) of other day i ($i \ne 1$) is denoted by $E_{\text{st,ini},i}$, which is determined by the storage controller. The full energy capacity of the energy storage system is $E_{\text{st,full}}$.

A. Storage Control Optimization at the Beginning of a Billing Period

We introduce the storage control optimization at the beginning of a billing period (i.e., at time 00:00 of day $i = 1$), in order to achieve a desirable balance between the expected Cost_E and expected Cost_D values. At that time, we have $\text{Peak}_k = 0$ for $1 \le k \le N$. The storage controller is only aware of the PV power generation and load power consumption profiles in the first day of the billing period, i.e., $P_{\text{pv},1}[j]$ and $P_{\text{load},1}[j]$ for $1 \le j \le 96$. The storage controller finds the optimal $P_{\text{st,in},1}[j]$ profile for $1 \le j \le 96$. The objective of the storage controller is to minimize the estimated total electricity cost in the billing period. Then the *O*ptimal *S*torage *C*ontrol problem performed at the *B*eginning of a billing period (the OSC-B problem) is formally described as follows.

1) OSC-B Problem Formulation: ***Given*** the PV power generation and load power consumption profiles of the first day in the billing period, i.e., $P_{\text{pv},1}[j]$ and $P_{\text{load},1}[j]$ for $1 \le j \le 96$, the initial storage energy $E_{\text{st,ini},1}$ at time 00:00, and full energy capacity $E_{\text{st,full}}$.

Find the optimal $P_{\text{st,in},1}[j]$ profile for $1 \le j \le 96$.

Minimize the estimated total electricity cost in the billing period, which is given by

$$\begin{aligned}&\text{Cost}_D + \text{Cost}_E \\ &= 30 \cdot \sum_{j=1}^{96} \text{Price}_E[j] \cdot P_{\text{grid},1}[j] \cdot D \\ &\quad + \sum_{k=1}^{N} \text{Price}_{D,k} \cdot \max\left(\text{Peak}_k, \max_{j \in \boldsymbol{S}_k} P_{\text{grid},1}[j]\right). \end{aligned} \tag{8}$$

Subject to the following constraints:
For each $1 \le j \le 96$

$$-P_{\max,c} \le P_{\text{st,in},1}[j] \le P_{\max,d} \tag{9}$$

$$0 \le E_{\text{st,ini},1} - \sum_{l=1}^{j} P_{\text{st,in},1}[l] \cdot D \le E_{\text{st,full}} \tag{10}$$

$$E_{\text{st,ini},1} - \sum_{j=1}^{96} P_{\text{st,in},1}[j] \cdot D \ge E_{\text{st,ini},1}. \tag{11}$$

In the OSC-B problem formulation, the objective function (8) is the estimated total electricity cost in the whole billing period, where we use the PV and load profiles of the first day, i.e., $P_{\text{pv},1}[j]$ and $P_{\text{load},1}[j]$ for $1 \le j \le 96$, as a representation for the whole billing period. This is because the storage controller is only aware of the PV power generation and load power consumption profiles in the first day. Constraint (9) represents

the restrictions on the maximum allowable amount of power flowing into and out of the storage system during charging and discharging, respectively. Constraint (10) ensures that the storage energy can never become less than zero or exceed a maximum value $E_{\text{st,full}}$ throughout the day. Finally, constraint (11) ensures that the remaining storage energy at the end of day, which is required for performing peak power shaving on the next day, is no less than the initial value $E_{\text{st,ini},1}$.

The OSC-B problem is a standard convex optimization problem due to the following two reasons.

1) The objective function (8) is a convex objective function because the pointwise maximum function of a set of convex functions is still a convex function.
2) The other constraints are all convex (or linear) inequality constraints of optimization variables.

Although the OSC-B problem is formulated as a convex optimization problem, and therefore, it can be solved optimally with a polynomial time complexity using convex optimization algorithms [22], it is difficult to directly solve the OSC-B problem using standard convex optimization tools such as CVX [23] or the *fmincon* function in MATLAB. This is because the function $P_{\text{grid},i}[j] = f_{\text{grid}}\left(P_{\text{st,in},i}[j]\right)$ is nondifferentiable at several points, and typical convex optimization tools only accept differentiable objective functions. To address this issue, we use a piecewise linear function to approximate the function $f_{\text{grid}}\left(P_{\text{st,in},i}[j]\right)$, and then transform the OSC-B problem into a linear programming problem (note that all the constraints are linear constraints), which could be optimally solved using standard optimization tools in polynomial time complexity. Details are omitted due to space limitation. Similar method will also be applied to the optimal storage problem as shall be discussed in Section IV-B.

B. Storage Control Optimization at the Beginning of the Other Days

We introduce the storage control optimization at the beginning of the other days in the billing period (i.e., days 2, 3, and so on). Suppose that we are at the beginning of the ith day of the billing period of interest. At that time, the Peak_k values may not be zero any more. The storage controller is aware of the PV power generation and load power consumption profiles in the ith day, i.e., $P_{\text{pv},i}[j]$ and $P_{\text{load},i}[j]$ for $1 \le j \le 96$. The storage controller derives the optimal $P_{\text{st,in},i}[j]$ profile for $1 \le j \le 96$. The objective of the storage controller is to minimize *the increase of the electricity cost* in the ith day of the billing period, as will be formally described below. The *O*ptimal *S*torage *C*ontrol problem performed at the beginning of the *O*ther days in the billing period (the OSC-O problem) is formally described as follows.

1) OSC-O Problem Formulation: ***Given*** the PV power generation and load power consumption profiles of the ith day in the billing period, i.e., $P_{\text{pv},i}[j]$ and $P_{\text{load},i}[j]$ for $1 \le j \le 96$, and the initial storage energy $E_{\text{st,ini},i}$ at time 00:00.

Find the optimal $P_{\text{st,in},i}[j]$ profile for $1 \le j \le 96$.

Minimize the increase in the electricity cost in the ith day, which is given by

$$\sum_{j=1}^{96} \text{Price}_E[j] \cdot P_{\text{grid},i}[j] \cdot D + \sum_{k=1}^{N} \text{Price}_{D,k} \cdot \left(\max\left(\text{Peak}_k, \max_{j \in \boldsymbol{S}_k} P_{\text{grid},i}[j] \right) - \text{Peak}_k \right) \tag{12}$$

or equivalently, minimize

$$\sum_{j=1}^{96} \text{Price}_E[j] \cdot P_{\text{grid},i}[j] \cdot D + \sum_{k=1}^{N} \text{Price}_{D,k} \cdot \max\left(\text{Peak}_k, \max_{j \in \boldsymbol{S}_k} P_{\text{grid},i}[j] \right). \tag{13}$$

Subject to the following constraints:
For each $1 \le j \le 96$

$$-P_{\max,c} \le P_{\text{st,in},i}[j] \le P_{\max,d} \tag{14}$$

$$0 \le E_{\text{st,ini},i} - \sum_{l=1}^{j} P_{\text{st,in},i}[l] \cdot D \le E_{\text{st,full}} \tag{15}$$

$$E_{\text{st,ini},i} - \sum_{j=1}^{96} P_{\text{st,in},i}[j] \cdot D \ge E_{\text{st,res}}. \tag{16}$$

In the OSC-O problem formulation, the objective function (12) is the increase of the electricity cost in the ith day of the billing period of interest. The objective function comprised two parts: 1) the energy price-induced electricity cost in the ith day of the billing period, given by the first term of (12) and 2) the increase in the demand price-induced electricity cost in the billing period of interest, given by the second term of (12). The constraints in the OSC-O problem are similar to the constraints in the OSC-B problem discussed in Section IV-A. However, in constraint (16), the minimum storage energy at the end of the day is set to be $E_{\text{st,res}}$, which is adaptively updated using a reinforcement learning technique [24]. We will introduce the learning of the optimal $E_{\text{st,res}}$ value in Section IV-C.

Again, similar to the OSC-B problem, the OSC-O problem has convex objective function (12), and linear inequality constraints (14)–(16), of optimization variables. Therefore, the OSC-O problem can also be optimally solved in polynomial time complexity using standard convex optimization methods [22], [23].

C. Reinforcement Learning Technique to Derive the Optimal Amount of Residual Energy

The limitation on residual energy is critical for the performance of storage control algorithm. A large amount of residual energy (suppose the battery is nearly fully charged) will degrade the capability of the storage module to store future redundant energy, whereas a small amount of residual energy

(suppose the battery is nearly depleted) will degrade the capability of the storage module to perform peak shaving. Hence, the most critical task is the evaluation and selection of the $E_{\text{st,res}}$ value.

We propose a reinforcement learning-based technique [24] to adaptively derive the optimal value of $E_{\text{st,res}}$ along with system operation. A reinforcement learning framework has a set of states $\boldsymbol{S}$ and a set of actions $\boldsymbol{A}$ to choose at each state. In this problem, a state $s \in \boldsymbol{S}$ is a specific amount of remaining energy at the beginning of each day i (i.e., the residual energy for the previous day), whereas an action $a \in \boldsymbol{A}$ corresponds to a specific $E_{\text{st,res}}$ value at the end of the ith day. In reinforcement learning, we maintain a value function $Q(s,a)$ for each state-action pair (s,a). $Q(s,a)$ stores the *estimation of the expected discounted total electricity cost* when starting at state s and taking action a [24]. At the beginning of each day i (suppose the state is s),[3] the storage controller selects the optimal action a (which corresponds to a specific $E_{\text{st,res}}$ value) with the smallest $Q(s,a)$ value, and consequently, performs optimization of storage charging/discharging (i.e., the OSC-O optimization). At the end of the ith day, the storage controller evaluates the value function $Q(s,a)$ of state-action pair (s,a) using the following value updating rule:

$$Q(s,a) \leftarrow (1-\alpha)\cdot Q(s,a) + \alpha \cdot \left(\text{Cost} + \gamma \cdot \min_{a'} Q(s',a')\right) \tag{17}$$

where s' is the observed next state at the end of the ith day, Cost is the cost increase in the ith day as defined in (12), γ is the discount factor, and α is a learning parameter. This learning technique is called Q-learning [24], and it produces the optimal $E_{\text{st,res}}$ value along with system operation. According to [24] and our experiments, we can get good learning results when α is set around 0.05–0.15 and γ is set around 0.85–0.95. Detailed procedure of the learning algorithm in each day i is provided in Algorithm 1.

Algorithm 1. Reinforcement learning-based optimization of the residual energy $E_{\text{st,res}}$

At the beginning of each day i (suppose we are currently in state s):
- Choose action a (which corresponds to a specific $E_{\text{st,res}}$ value) with the smallest $Q(s,a)$ value.
- Perform optimization of storage charging/discharging (i.e., the OSC-O optimization) correspondingly.

We arrive at the end of day i (suppose the observed next state is s'):
- Evaluate the value function $Q(s,a)$ of state-action pair (s,a) as shown in Eqn. (17).

V. Experimental Results

In this section, we present the simulation results on the effectiveness of the proposed accurate component model-based near-optimal residential storage control algorithm. The PV power profiles used in our experiments are measured at Duffield, VA, in the year 2007, whereas the electric load data come from the Baltimore Gas and Electric Company, also measured in the year 2007 [25]. We add some random peaks to the electric load profiles. The algorithm is implemented in MATLAB and executes on a computer with an Intel Core i7-3770 CPU running at 3.40 GHz.

[3]Note that this learning procedure is not used in the first day of a month, since we do not incorporate $E_{\text{st,res}}$ in the OSC-B problem.

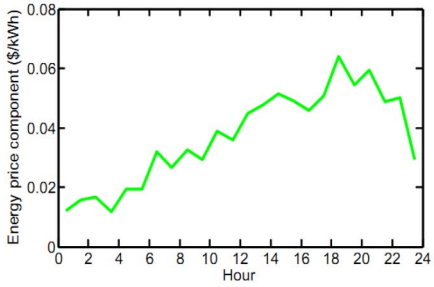

Fig. 4. Daily energy price component in the second type of electricity price function.

We use two types of electricity price functions. The first type of electricity price function is a real price function similar to [12] and [13], given as follows. The energy price component is given by: 0.01879 $/kWh during 00:00 to 09:59 and 20:00 to 23:59, 0.03952 $/kWh during 10:00 to 12:59 and 17:00 to 19:59, 0.04679 $/kWh during 13:00 to 16:59. For the monthly demand price component, there are three price periods in a day: 1) the "high peak" period from 13:00 to 16:59, with demand price of 9.00 $/kW; 2) the "low peak" period from 10:00 to 12:59 and from 17:00 to 19:59, with demand price of 3.25 $/kW; and 3) the "overall" period from 00:00 to 23:59 (the whole day), with demand price of 5.00 $/kW. The second type is a synthesized electricity price function. The energy price component over a day is demonstrated in Fig. 4. For the monthly demand price component, we consider only one "high peak" period from 18:00 to 21:59 with demand price of 9.00 $/kW, whereas the rest is "low peak" period.

We compare the performances (in terms of actual cost and cost-saving capabilities as shall be defined later) of the proposed near-optimal storage control algorithm with the baseline algorithm. The baseline algorithm charges the storage system from the Grid during the "off peak" period (00:00 to 09:59 and 20:00 to 23:59 in the first type of electricity price function or 00:00 to 17:59 and 22:00 to 23:59 in the second type of electricity price function) with constant charging power, and distributes energy stored in the storage system evenly in the "high peak" period. We define the *cost-saving capability* of a storage control algorithm (the proposed algorithm or the baseline algorithm) to be the total cost saving over a billing period due to the additional storage system, compared with the same residential Smart Grid user equipped only with the PV system.

A. Simulation Results Using the First Type of Electricity Price Function

First, we show experimental results based on the first type of electricity price function. Fig. 5 illustrates the comparison

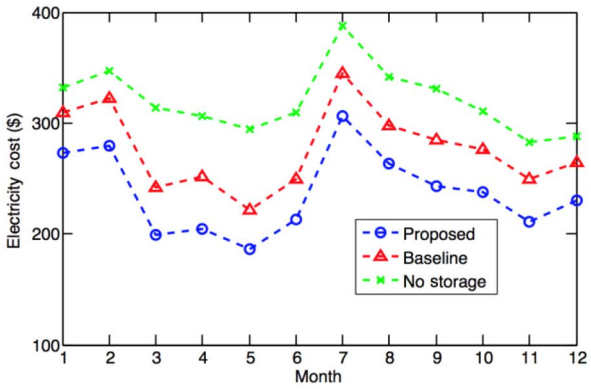

Fig. 5. Comparison results on the actual electricity cost on every month throughout a year.

TABLE I
IMPROVEMENT IN COST-SAVING CAPABILITY OF THE PROPOSED ALGORITHM WITH LEARNING-BASED OPTIMIZATION OF RESIDUAL ENERGY COMPARED WITH THE BASELINE ALGORITHM, WHEN THE STORAGE CAPACITY IS 45 AH, UNDER THE FIRST TYPE OF PRICE FUNCTION

Month	Jan.	Feb.	Mar.	Apr.
Improvement	164%	167%	60%	90%
Month	May	Jun.	Jul.	Aug.
Improvement	55%	59%	67%	85%
Month	Sep.	Oct.	Nov.	Dec.
Improvement	79%	81%	145%	87%

results on the actual electricity cost on every month throughout a year, among the proposed near-optimal storage control algorithm with learning-based optimization of residual energy, the baseline algorithm, and the residential user equipped only with the PV system (no energy storage). The capacity of the storage system is set to be 45 Ah. We can observe that the proposed near-optimal residential storage control algorithm consistently outperforms the baseline algorithm in energy cost reductions.

For more quantitative results, Table I illustrates the comparison results on the cost-saving capabilities between the proposed near-optimal storage control algorithm and the baseline algorithm on every month throughout a year, when the capacity of the storage system is 45 Ah. The improvement in cost-saving capabilities using the proposed algorithm is provided in the table. Table II shows the comparison results on the same testing data when the capacity of the storage system is 60 Ah. Experimental results demonstrate that the optimal amount of residual energy at the end of each day is around 20%–40% of the full energy capacity of the storage system. We can see from the two tables that the proposed near-optimal residential storage control algorithm consistently outperforms the baseline algorithm, with a maximum improvement of 191% (i.e., 2.91×) on the cost-saving capability (on February, 60-Ah storage capacity). Furthermore, it can be observed that the proposed storage control algorithm demonstrates more significant improvement on the cost-saving capability over the baseline system when the storage system has a capacity of 60 Ah. It also achieves

TABLE II
IMPROVEMENT IN COST-SAVING CAPABILITY OF THE PROPOSED ALGORITHM WITH LEARNING-BASED OPTIMIZATION OF RESIDUAL ENERGY COMPARED WITH THE BASELINE ALGORITHM, WHEN THE STORAGE CAPACITY IS 60 AH, UNDER THE FIRST TYPE OF PRICE FUNCTION

Month	Jan.	Feb.	Mar.	Apr.
Improvement	183%	191%	69%	97%
Month	May	Jun.	Jul.	Aug.
Improvement	52%	67%	77%	99%
Month	Sep.	Oct.	Nov.	Dec.
Improvement	87%	92%	159%	97%

TABLE III
IMPROVEMENT IN COST-SAVING CAPABILITY OF THE PROPOSED ALGORITHM WITH THE BASELINE ALGORITHM, WHEN THE STORAGE CAPACITY IS 60 AH, UNDER THE FIRST TYPE OF PRICE FUNCTION, AND ACCOUNTING FOR PREDICTION INACCURACIES

Month	Jan.	Feb.	Mar.	Apr.
Improvement	115%	101%	49%	86%
Month	May	Jun.	Jul.	Aug.
Improvement	38%	54%	26%	47%
Month	Sep.	Oct.	Nov.	Dec.
Improvement	91%	71%	47%	118%

higher cost-saving capability during the winter than during the summer. The reason is that the peak load power consumption generally occurs in the "high peak" price period in the summer, and therefore, the baseline algorithm achieves relatively higher performance by distributing the storage energy only in the "high peak" periods.

Next, we consider the effect of prediction inaccuracies in PV power generation and load power consumption predictions. As reported in [6], the above prediction inaccuracies can be lower than 8%. Hence, we assume 8% prediction inaccuracies of PV power generation and load power consumption predictions, and illustrate in Table III the comparison results on the cost-saving capabilities between the proposed near-optimal storage control algorithm and the baseline algorithm on every month throughout a year (the storage capacity is 45 Ah). We can observe that the performance gains in Table III are generally lower than those in Table I (when prediction inaccuracies are not accounted for). But still, we can achieve up to 117.6% improvement in cost-saving capabilities when applying the proposed control algorithm.

B. Simulation Results Using the Second Type of Electricity Price Function

Next, we show experimental results based on the second type of electricity price function. We only show experimental results on the 60-Ah storage system due to space limitation. Table IV illustrates the comparison results on the cost-saving capabilities between the proposed near-optimal storage control algorithm with learning-based optimization of residual energy and the baseline algorithm on every month throughout a year. Experimental results demonstrate that in this case

TABLE IV
IMPROVEMENT IN COST-SAVING CAPABILITY OF THE PROPOSED ALGORITHM WITH LEARNING-BASED OPTIMIZATION OF RESIDUAL ENERGY COMPARED WITH THE BASELINE ALGORITHM, UNDER THE SECOND TYPE OF PRICE FUNCTION

Month	Jan.	Feb.	Mar.	Apr.
Improvement	36%	60%	42%	42%
Month	May	Jun.	Jul.	Aug.
Improvement	41%	24%	39%	46%
Month	Sep.	Oct.	Nov.	Dec.
Improvement	37%	23%	51%	72%

the optimal amount of residual energy at the end of each day is around 10%–20% of the full energy capacity of the storage system, which is less than that in the former case. Once again, the proposed near-optimal residential storage control algorithm consistently outperforms the baseline algorithm, with a maximum improvement of 72% on the cost-saving capability. However, one can notice that the improvement is less significant than the results on the first type of electricity price function. This is because the energy cost due to demand price component is less significant compared with that due to energy price component in this case, which will degrade the improvement achieved by the proposed near-optimal solution (because the proposed solution is the most effective in reducing cost due to the demand price component).

VI. CONCLUSION

In this paper, we address the problem of integrating residential PV power generation and storage systems into the Smart Grid for simultaneous peak power shaving and total electricity cost minimization over a billing period, making use of the dynamic energy pricing models. The residential storage control should effectively mitigate the inevitable prediction errors and properly account for the energy loss in storage charging/discharging and in power conversion circuitries. Based on the PV power generation and load power consumption prediction methods in our previous papers, we propose an accurate component model-based near-optimal storage control algorithm accounting for these aspects. We effectively implement the near-optimal storage control algorithm by solving a convex optimization problem at the beginning of each day with polynomial time complexity. We adopt reinforcement learning technique to adaptively determine the amount of residue energy in the energy storage module at the end of each day in a billing period.

REFERENCES

[1] Y. Wang, X. Lin, and M. Pedram, "Accurate component model based optimal control for energy storage systems in households with photovoltaic modules," in *Proc. IEEE Green Technol. Conf. (GTC)*, 2013, pp. 28–34.

[2] L. D. Kannberg *et al.*, "GridWise^{TM}: The benefits of a transformed energy system," Pacific Northwest Nat. Lab., Richland, WA, USA, PNNL-14396, Sep. 2003.

[3] S. M. Amin and B. F. Wollenberg, "Toward a smart grid: Power delivery for the 21st century," *IEEE Power Energy Mag.*, vol. 3, no. 5, pp. 34–41, Sep./Oct. 2005.

[4] S. Kishore and L. V. Snyder, "Control mechanisms for residential electricity demand in SmartGrids," in *Proc. IEEE Smart Grid Commun.*, 2010, pp. 443–448.

[5] S. Caron and G. Kesidis, "Incentive-based energy consumption scheduling algorithms for the Smart Grid," in *Proc. IEEE Smart Grid Commun.*, 2010, pp. 391–396.

[6] Y. Wang, S. Yue, L. Kerofsky, S. Deshpande, and M. Pedram, "A hierarchical control algorithm for managing electrical energy storage systems in homes equipped with PV power generation," in *Proc. IEEE Green Technol. Conf. (GTC)*, 2012, pp. 1–6.

[7] A. Mohd, E. Ortjohann, A. Schmelter, N. Hamsic, and D. Morton, "Challenges in integrating distributed energy storage systems into future smart grid," in *Proc. Int. Symp. Ind. Electron. (ISIE)*, 2008, pp. 1627–1632.

[8] I. Koutsopoulos, V. Hatzi, and L. Tassiulas, "Optimal energy storage control policies for the smart power grid," in *Proc. IEEE Int. Conf. Smart Grid Commun.*, Oct. 2011, pp. 475–480.

[9] T. Cui, Y. Wang, H. Goudarzi, S. Nazarian, and M. Pedram, "Profit maximization for utility companies in an oligopolistic energy market with dynamic prices," in *Proc. Online Green Commun. Conf.*, 2012, pp. 86–91.

[10] T. Esram, J. Kimball, P. Krein, P. Chapman, and P. Midya, "Dynamic maximum power point tracking of photovoltaic arrays using ripple correlation control," *IEEE Trans. Power Electron.*, vol. 21, no. 5, pp. 1282–1291, Sep. 2006.

[11] Y. Kim, N. Chang, Y. Wang, and M. Pedram, "Maximum power transfer tracking for a photovoltaic-supercapacitor energy system," in *Proc. Int. Symp. Low Power Electron. Des. (ISLPED)*, 2010, pp. 307–312.

[12] Los Angeles Department of Water & Power. (2011). *Electric Rates* [Online]. Available: http://www.ladwp.com/ladwp/cms/ladwp001752.jsp

[13] Consolidated Edison Company of New York, Inc. (2012). "Service classification no. 1—Residential and religious."

[14] T. Hiyama and K. Kitabayashi, "Neural network based estimation of maximum power generation from PV module using environmental information," *IEEE Trans. Energy Convers.*, vol. 12, no. 3, pp. 241–247, Sep. 1997.

[15] L. Martin, L. F. Zarzalejo, J. Polo, A. Navarro, R. Marchante, and M. Cony, "Prediction of global solar irradiance based on time series analysis: Application to solar thermal power plants energy production planning," *Sol. Energy*, vol. 84, no. 10, pp. 1772–1781, Oct. 2010.

[16] T. Senjyu, H. Takara, K. Uezato, and T. Funabashi, "One-hour-ahead load forecasting using neural network," *IEEE Trans. Power Syst.*, vol. 17, no. 1, pp. 113–118, Feb. 2002.

[17] C. Chen, B. Das, and D. J. Cook, "Energy prediction based on resident's activity," in *Proc. Int. Workshop Knowl. Discovery Sens. Data (SensorKDD'10)*, 2010, pp. 1–7.

[18] L. Wei and Z.-H. Han, "Short-term power load forecasting using improved ant colony clustering," in *Proc. Int. Workshop Knowl. Discov. Data Min. (WKDD)*, 2008, pp. 221–224.

[19] D. Linden and T. B. Reddy, *Handbook of Batteries*. New York, NY, USA: McGraw-Hill, 2001.

[20] M. Pedram, N. Chang, Y. Kim, and Y. Wang, "Hybrid electrical energy storage systems," in *Proc. Int. Symp. Low Power Electron. Des. (ISLPED)*, 2010, pp. 363–368.

[21] D. Shin, Y. Wang, Y. Kim, J. Seo, N. Chang, and M. Pedram, "Battery-supercapacitor hybrid system for high-rate pulsed load applications," in *Proc. Des. Autom. Test Eur. (DATE)*, 2011, pp. 1–4.

[22] S. Boyd and L. Vandenberghe, *Convex Optimization*. Cambridge, U.K.: Cambridge Univ. Press, 2004.

[23] M. Grant and S. Boyd. (2011, February). *CVX: Matlab Software for Disciplined Convex Programming, Version 1.21* [Online]. Available: http://cvxr.com/cvx

[24] R. S. Sutton and A. G. Barto, *Reinforcement Learning: An Introduction*. Cambridge, MA, USA: MIT Press, 1998.

[25] Baltimore Gas and Electric Company. (2011). *Historical Load Data* [Online]. Available: https://supplier.bge.com/LoadProfiles_EnergySettlement/historicalloaddata.htm

[26] M. Nymand and M. Andersen, "High-efficiency isolated boost dc-dc converter for high-power low-voltage fuel-cell applications," *IEEE Trans. Ind. Electron.*, vol. 57, no. 2, pp. 505–514, Feb. 2010.

[27] S. Park, Y. Wang, Y. Kim, N. Chang, and M. Pedram, "Battery management for grid-connected PV systems with a battery," in *Proc. ACM/IEEE Int. Symp. Low Power Electron. Des. (ISLPED)*, 2012, pp. 115–120.

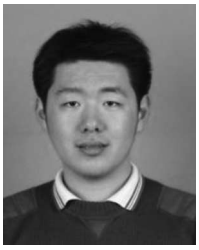

Yanzhi Wang (S'12) received the B.S. degree with distinction in electronic engineering from Tsinghua University, Beijing, China, in 2009, and the Ph.D. degree in electrical engineering from the University of Southern California, Los Angeles, CA, USA, in 2014.

He is currently a Postdoctoral Research Associate and (Part-Time) Lecturer with the University of Southern California. He will be joining the Department of Electrical Engineering and Computer Science, Syracuse University, Syracuse, NY, USA, as an Assistant Professor, in Fall 2015. His research interests include system-level power management, low-power near-threshold computing, applications of energy storage and energy generation systems, etc. He has authored more than 100 papers in these areas.

Dr. Wang received the Best Paper awards at the 2014 IEEE International Symposium on VLSI (ISVLSI) and the 2014 IEEE/ACM International Symposium on Low Power Electronics Design (ISLPED), and the Top Paper award at the 2014 IEEE Cloud Computing Conference (IEEE Cloud).

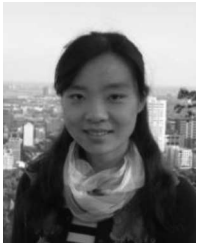

Xue Lin (S'12) received the B.S. degree in electronic engineering from Tsinghua University, Beijing, China, in 2009. She is currently pursuing the Ph.D. degree in electrical engineering at the University of Southern California, Los Angeles, CA, USA.

She has been working on power management of photovoltaic (PV) systems, near-threshold computing of FinFET circuits, task scheduling in real-time and mobile systems, and power management of energy storage systems and electric vehicles. She has authored around 50 papers in these areas.

Ms. Lin received the Best Paper award at the 2014 IEEE International Symposium on VLSI (ISVLSI), and the Top Paper award at the 2014 IEEE Cloud Computing Conference (IEEE Cloud).

Massoud Pedram (F'01) received the Ph.D. degree in electrical engineering and computer sciences from the University of California, Berkeley, CA, USA, in 1991.

He is the Stephen and Etta Varra Professor with the Ming Hsieh Department of Electrical Engineering, University of Southern California, Los Angeles, CA, USA. He holds 10 U.S. patents and has authored four books, 13 book chapters, and more than 140 archival and 380 conference papers. His research interests include low power electronics, energy-efficient processing, and cloud computing to photovoltaic cell power generation, energy storage, and power conversion, and from RT-level optimization of VLSI circuits to synthesis and physical design of quantum circuits.

Dr. Pedram is an ACM Distinguished Scientist, and currently serves as the Editor-in-Chief of the *ACM Transactions on Design Automation of Electronic Systems* and the IEEE JOURNAL ON EMERGING AND SELECTED TOPICS IN CIRCUITS AND SYSTEMS. He has also served on the Technical Program Committee of a number of premiere conferences in his field and was the founding Technical Program Co-Chair of the 1996 International Symposium on Low Power Electronics and Design and the Technical Program Chair of the 2002 International Symposium on Physical Design. He was a recipient of the 1996 Presidential Early Career Award for Scientists and Engineers. He and his students have received seven conference and two IEEE TRANSACTIONS Best Paper Awards.